

1 **Brain age prediction using fMRI network coupling in youths and associations with**
2 **psychiatric symptoms**

3
4 Martina J. Lund^{1*}, Dag Alnæs^{1,2}, Ann-Marie de Lange^{1,3,4}, Ole A. Andreassen^{1,5}, Lars T.
5 Westlye^{1,5,6}, Tobias Kaufmann^{1,7*}.

6
7 ¹ Norwegian Centre for Mental Disorders Research (NORMENT), Division of Mental Health
8 and Addiction, Oslo University Hospital, and Institute of Clinical Medicine, University of
9 Oslo, Norway

10 ² Bjørknes College, Oslo, Norway

11 ³ LREN, Centre for Research in Neurosciences - Department of Clinical Neurosciences,
12 CHUV and University of Lausanne, Lausanne, Switzerland

13 ⁴ Department of Psychiatry, University of Oxford, Oxford, UK

14 ⁵ KG Jebsen Centre for neurodevelopmental disorders, University of Oslo, Oslo, Norway

15 ⁶ Department of Psychology, University of Oslo, Oslo, Norway

16 ⁷ Department of Psychiatry and Psychotherapy, University of Tübingen, Germany

17
18 * Corresponding authors:

19 Martina J. Lund and Tobias Kaufmann, PhD

20 Email: m.j.lund@medisin.uio.no, tobias.kaufmann@medisin.uio.no

21 Postal address: OUS, PoBox 4956 Nydalen, 0424 Oslo, Norway

22 Telephone: +47 23 02 73 50, Fax: +47 23 02 73 33

23
24
25 Counts:

26 Abstract: 256 words

27 Main text body: 4383 words

28 Figures: 4

29
30 Keywords:

31 Machine learning

32 Brain age

33 Development

34 Resting-state fMRI

35 The Healthy Brain Network

36 The Philadelphia Neurodevelopmental Cohort

45 **Abstract**

46 Objective: Magnetic resonance imaging (MRI) has shown that estimated brain age is deviant
47 from chronological age in various common brain disorders. Brain age estimation could be
48 useful for investigating patterns of brain maturation and integrity, aiding to elucidate brain
49 mechanisms underlying these heterogeneous conditions. Here, we examined functional brain
50 age in two large samples of children and adolescents and its relation to mental health.

51 Methods: We used resting-state fMRI data from the Philadelphia Neurodevelopmental Cohort
52 (PNC; n=1126, age range 8-22 years) to estimate functional connectivity between brain
53 networks, and utilized these as features for brain age prediction. We applied the prediction
54 model to 1387 individuals (age range 8-22 years) in the Healthy Brain Network sample
55 (HBN). In addition, we estimated brain age in PNC using a cross-validation framework. Next,
56 we tested for associations between brain age gap and various aspects of psychopathology and
57 cognitive performance.

58 Results: Our model was able to predict age in the independent test samples, with a model
59 performance of $r=0.54$ for the HBN test set, supporting consistency in functional connectivity
60 patterns between samples and scanners. Linear models revealed a significant association
61 between brain age gap and psychopathology in PNC, where individuals with a lower
62 estimated brain age, had a higher overall symptom burden. These associations were not
63 replicated in HBN.

64 Discussion: Our findings support the use of brain age prediction from fMRI-based
65 connectivity. While requiring further extensions and validations, the approach may be
66 instrumental for detecting brain phenotypes related to intrinsic connectivity and could assist
67 in characterizing risk in non-typically developing populations.

68

69 **Introduction**

70 Psychiatric disorders are complex disorders with substantial heterogeneity in symptoms and
71 prognosis, and comorbidities are usually the rule rather than the exception (Craddock &
72 Owen, 2010; Krueger & Bezdjian, 2009; Nemeroff, 2002). This heterogeneity is also apparent
73 in the brain, and magnetic resonance imaging (MRI) studies suggest greater structural
74 variability among patients compared to healthy controls (Alnaes et al., 2019). This poses
75 substantial challenges for elucidating the brain mechanisms underlying these disorders, and
76 observed effects for neuromarkers are commonly minor in mental health research (Jollans &
77 Whelan, 2018; Linden, 2012; Paulus & Thompson, 2019). This is further exacerbated by the
78 lack of strong mapping between the current symptom-based nosology and the underlying
79 biology (Owen, 2014). Given this multivariate complexity, studies have increasingly turned to
80 machine-learning approaches that can utilize large amounts of data to provide individual-level
81 predictions by the use of dimensionality reduction and pattern recognition (Cao & Schwarz,
82 2020; Mansourvar M., Wiil U.K., & C., 2020). The aim is to provide a better mapping of
83 brain imaging data to symptoms, cognition and behavior.

84 One avenue provided by machine learning is its utility to map the substantial anatomical and
85 functional changes that the brain undergoes throughout life. Training machine learning
86 models to predict chronological age from brain imaging data allows us to derive the apparent
87 age of the brain - referred to as 'brain age' - and its deviation from chronological age, referred
88 to as the 'brain age gap' (Franke, Ziegler, Kloppel, Gaser, & Alzheimer's Disease
89 Neuroimaging, 2010). Depending on the modality that is fed into the model, such estimates of
90 apparent brain age can reflect different neurophysiology such as anatomical brain age (Franke
91 et al., 2010) and functional brain age (Dosenbach et al., 2010). It is also possible to study this
92 process for specific parts of the brain to gain insights into region specific alterations
93 (Kaufmann et al., 2019). Studies that have applied brain age prediction to clinical data have

94 shown that adults with psychiatric disorders such as schizophrenia, have a brain that appears
95 older and age faster compared to people without mental disorders (Schnack et al., 2016).
96 Regional differences in brain age gaps between different disorders have also been observed.
97 For instance, individuals with schizophrenia were found to have most pronounced age gap for
98 the frontal lobe, while increased cerebellar-subcortical age gaps was found to be predominant
99 in dementia and multiple sclerosis (Kaufmann et al., 2019).

100 As the mechanisms of psychiatric disorders are assumed to have a strong neurodevelopmental
101 component (Insel, 2010) and deviant developmental trajectories have been observed in
102 imaging data of youths with early signs of psychiatric disorders (Besenek, 2020; Chung et al.,
103 2018; Collin et al., 2020; Kaufmann et al., 2017; Lian et al., 2018; Saito et al., 2020),
104 estimating brain age gap as a proxy for maturation in young individuals may provide further
105 insights into the early phases of the disorders. Indeed, an increase in anatomical brain age
106 gaps has been observed in association with psychopathology in children and adolescents
107 (Chung et al., 2018; Cropley et al., 2020; Franke, Luders, May, Wilke, & Gaser, 2012).
108 Anatomical brain age during neurodevelopment has also been found to be dependent on sex
109 and to be partly heritable (Brouwer et al., 2020). Additionally, functional measures have been
110 used for brain age prediction in development (Dosenbach et al., 2010; Kassani, Gossman, &
111 Wang, 2020; Li, Satterthwaite, & Fan, 2018; Rudolph et al., 2017; Truelove-Hill et al., 2020;
112 Zhai & Li, 2019), but the implications of functional brain age gaps have yet to be further
113 explored across neurodevelopmental disorders in large samples of children and adolescents.

114 Here, we used functional MRI data from 1126 individuals aged 8-22 years to train a machine
115 learning model to estimate brain age. We applied the resulting model to independent
116 functional imaging data of 1387 youths aged 8 to 22 to derive functional brain age gaps. Next,
117 we used linear models to test for associations between brain age gap and psychopathology in

118 youths, using behavioral measures constructed from diagnostic criterion for selected DSM-5
119 disorders. Based on previous findings, we expected to observe an association between delayed
120 functional brain development and psychopathology on top of differences related to sex and
121 cognitive test performance.

122

123 **Methods**

124 **Study samples**

125 The Healthy Brain Network (HBN) study sample is an initiative coordinated by the Child
126 Mind Institute, where the aim is to provide a unique understanding of the time period when
127 psychiatric disorders emerge (Alexander et al., 2017). Age range for inclusion of participants
128 is 5-21 years. Individuals are included in the New York area through announcements
129 circulated to community members, educators, and local care providers. In addition,
130 information via email lists was sent out and spread on parent events, where children with
131 clinical concerns were encouraged to take part in this study (Alexander et al., 2017). The
132 participants go through an extensive assessment package where MRI, genetics,
133 electroencephalography (EEG), eye-tracking, biological testing, actigraphy, voice and video
134 interviews are incorporated. In addition, the assessments include a neuropsychological battery
135 and rich information on cognitive, lifestyle, behavioral and psychiatric factors (Alexander et
136 al., 2017). Exclusion criteria comprise serious neurological disorders, neurodegenerative
137 disorders, acute encephalopathy, hearing or visual impairment, lifetime substance abuse that
138 required chemical replacement therapy/acute intoxication at time of study, recent diagnosis of
139 a severe mental disorder or manic/psychotic episode within the last 6 months that did not
140 receive continuing treatment. The onset of suicidality/homicidality where there is no current
141 treatment was also an exclusion criterion (Alexander et al., 2017). Participants over the age of
142 18 years gave signed informed consent, and legal guardians signed informed consent for

143 participants under the age of 18, in addition to participants giving a written assent (Alexander
144 et al., 2017). The Chesapeake Institutional Review Board approved the study ([https://www.
145 chesapeakeirb.com/](https://www.chesapeakeirb.com/)).

146

147 The Philadelphia Neurodevelopmental Cohort (PNC) is a research initiative funded by the
148 National Institutes of Mental Health (NIMH) that aims to describe the interaction between the
149 brain, behavior and genetics (Satterthwaite et al., 2016). The PNC participants were selected
150 after stratification by sex, age and ethnicity (Satterthwaite et al., 2014) from a larger sample
151 of children enrolled in a genetic study at the Center of Applied Genomics, at the Children's
152 Hospital of Philadelphia. They were included after they had been to a primary care facility
153 that was CHOP-affiliated in the Delaware Valley. The sample includes individuals with
154 different medical conditions, varying from a well-child visit and minor problems to
155 individuals with more complicated illnesses, however, individuals with medical problems that
156 could affect brain function were excluded (Satterthwaite et al., 2016). The inclusion criteria
157 comprised 1) ability to provide signed informed consent (parental consent was acquired for
158 participants under age 18), 2) English language proficiency, and 3) physical and cognitive
159 ability to participate in computerized clinical assessment and neurocognitive testing
160 (Satterthwaite et al., 2014). Participants underwent a structured neuropsychiatric interview in
161 addition to completion of the Computerized Neurocognitive Battery (CNB) (Satterthwaite et
162 al., 2014). The University of Pennsylvania and CHOP Institutional Review Boards approved
163 the study (Satterthwaite et al., 2016).

164

165 MRI acquisition

166 HBN: MRI scans were acquired at 3 sites; Rutgers University Brain Imaging Center
167 (RUBIC), Citigroup Biomedical Imaging Center (CBIC) and a mobile scanner placed in

168 Staten Island. Rutgers used a Siemens 3T Trim Tio scanner, while CBIC deployed a Siemens
169 3T Prisma. For RUBIC and CBIC, structural MRI data was acquired with a repeated 3D T1-
170 weighted sequence (TR: 2.5 s, TE: 3.15 ms, FA: 8°, FOV: 256 mm, slice thickness: 0.8 mm,
171 slices: 224). In addition, CBIC acquired a structural scan based on ABCD study protocol with
172 the following parameters; TR: 2.5 s, TE: 2.88 ms, FA: 8°, FOV: 256 mm, slice thickness: 1
173 mm, slices: 176. Resting- state blood-oxygen-level-dependent (BOLD) fMRI data was
174 acquired by means of a T2*-weighted BOLD echo-planar imaging (EPI) sequence with a
175 repetition time (TR) of 800ms, echo time (TE) of 30ms, multiband acceleration factor = 6,
176 number of slices: 60, and 375 repetitions and voxel size= 2.4×2.4×2.4 mm. Further, the
177 mobile scanner located in Staten Island employed a 1.5T Siemens Avanto system operational
178 with 45 mT/m gradients (Alexander et al., 2017), using these parameters for T1w data; TR:
179 2730 ms, TE1: 1.64ms, TE2: 3.5ms, TE3: 5.36 ms, TE4: 7.22 ms, multiband acceleration
180 factor = 3, FA: 7°, FOV: 256 mm, slice thickness: 1 mm, slices: 176. And for fMRI; TR:
181 1.45s, TE: 40 ms, number of volumes: 420, slices: 54, resolution: 2.5×2.5×2.5 mm
182 (http://fcon_1000.projects.nitrc.org/indi/cmi_healthy_brain_network/MRI%20Protocol.html).

183

184 PNC: A 3D T1-weighted magnetization prepared rapid acquisition gradient echo (MPRAGE)
185 sequence was obtained with a TR of 1.81 s, a TE of 3.5 ms, while FA: 9°, FOV: 240 × 180
186 mm, slice thickness: 1 mm, and number of slices: 160, and used for structural purposes. MRI
187 data was collected at the hospital of the University of Pennsylvania (Satterthwaite et al.,
188 2014). Resting-state BOLD fMRI data was collected by means of a T2*-weighted BOLD EPI
189 sequence with a TR of 3000 ms, TE of 32 ms, 46 number of slices, 124 repetitions and voxel
190 size= 3×3×3 mm (Satterthwaite et al., 2014).

191

192 Cognitive and psychiatric measures

193 HBN: In order to test for associations between brain age and cognition in the test sample, we
194 included the full-scale intelligence quotient (FSIQ) from the Wechsler Intelligence Scale for
195 Children (WISC-V) as a measure of cognitive abilities for HBN participants. This score
196 incorporates visual spatial, verbal comprehension, fluid reasoning, working memory, and
197 processing speed domains (Wechsler, 2003). Furthermore, to test for associations between
198 brain age and mental health we carried out a principal component analysis (PCA) on mental
199 health data, in line with our earlier work (Lund et al., 2020). Specifically, we used the
200 Extended Strengths and Weaknesses Assessment of Normal Behavior (E-SWAN), where
201 domains include depression, social anxiety, disruptive mood dysregulation disorder (DMDD),
202 and panic disorder (Alexander, Salum, Swanson, & Milham, 2020). This allowed us to assess
203 mental health symptoms on a continuum from healthy to patients to overcome the
204 shortcomings of the typical case-control dichotomy. We excluded three of the items which
205 related to panic disorder, as these questions had a high degree of missing values (90%). We
206 ended up with 62 items for the PCA. Further, excluding individuals with missing scores, we
207 had data for 2626 subjects for the PCA. We utilized the “prcomp” function in R to implement
208 the PCA. The resulting first component, referred to as the p-factor or pF (Caspi et al., 2013)
209 explained most variance across all the symptom domains of the ESWAN questionnaire
210 (43.6%) and was particularly associated with items linked to self-control and
211 depression/anxiety. We also included the second principal component (pF₂), which explained
212 11.3% of the variance and was associated with items describing mood dysregulation. For
213 both, pF and pF₂, a high score reflects lower mental health.

214

215 PNC: We made use of an already existing delineation of mental health data using PCA
216 (Alnæs et al., 2018) to derive a general psychopathology factor from clinical scores (Calkins

217 et al., 2015; Calkins et al., 2014), and to derive a general cognition component (Alnæs et al.,
218 2018) from various cognitive performance measures (Gur et al., 2014).

219

220 MRI processing and functional connectivity

221 MR data was collected by the study team of HBN (Alexander et al., 2017) and PNC

222 (Satterthwaite et al., 2016) and we processed both samples with the same pipeline.

223 Preprocessing included FSL MCFLIRT (Jenkinson, Bannister, Brady, & Smith, 2002) with

224 spatial smoothing (FWHM:6.0) and a high-pass filter cutoff of 100, non-aggressive ICA-

225 AROMA (Pruim, Mennes, Buitelaar, & Beckmann, 2015; Pruim, Mennes, van Rooij, et al.,

226 2015), followed by ICA FIX with a threshold of 20 (Griffanti et al., 2014; Salimi-Khorshidi et

227 al., 2014), described in earlier work (Kaufmann et al., 2017; Lund et al., 2021). Preprocessing

228 was followed by group level ICA using MELODIC group Independent Component Analysis

229 (Beckmann & Smith, 2004; Hyvärinen, 1999). For each sample and scanning site (1 for PNC;

230 N=1252, 3 for HBN; N=1685), we performed one group level ICA, followed by a meta-ICA

231 across all four sites, yielding ICs compliant across samples and sites. Due to the meta-ICA

232 framework, the number of components had to be pre-specified and we chose a model order of

233 100, as used in prior studies (de Lange et al., 2020; Miller et al., 2016; Smith et al., 2013).

234 After manual quality control through visual inspection of each IC, 53 components were

235 marked as artefactual while the rest of the components (47), were included for FSLNets

236 (<https://fsl.fmrib.ox.ac.uk/fsl/fslwiki/FSLNets>) to estimate correlations between each

237 functional network for each subject. In line with earlier work (Kaufmann et al., 2016), we

238 used a Ledoit & Wolf shrinkage estimator procedure for L2 Regularization (Ledoit & Wolf,

239 2003; Schäfer & Strimmer, 2005), which estimates regularization strength (λ) at the

240 individual level. Finally, we z-transformed the estimated correlations using Fisher's

241 transformation and used the upper triangle of the correlation matrix as a feature set for

242 machine learning, giving 1081 unique edges denoting the connection strength between two
243 IC's at the subject level.

244

245 The Shrinkage Estimation of Regression Coefficients (slm) function from the care package in
246 R was utilized for brain age prediction where default parameters were applied (Schäfer &
247 Strimmer, 2005). Using PNC data, we trained a model to predict age based on the 1081
248 correlations reflecting connection strengths between the 47 IC's referred to here as nodes. We
249 excluded the 10% (N=126) that scored highest on general psychopathology (pF) in order to
250 obtain a model based on healthy individuals, and used the data from the remaining 1126
251 subjects (age: 8.17–22.9 years, 47.1% males, mean: 15.2 years, sd: 3.54 years, median: 15.4
252 years) for model training. To validate model performance within PNC data, we performed a
253 10-fold cross validation, estimating age for each individual in each of the left-out folds while
254 training the model on the rest.

255

256 Afterwards, we tested the PNC model on HBN data (N=1387, age: 8.01–22.4 years, mean:
257 12.3 years, sd: 3.24 years, median: 11.5 years, 61.8% males, where information about sex was
258 missing for N= 30, and 298 subjects from the initial meta-ICA were excluded due to age
259 outside the training set range (age<8) or missing information about age at MRI). For each
260 individual in HBN, we estimated the brain age gap (BAG) by subtracting chronological age
261 from the estimated brain age.

262

263 Statistical analysis

264 We used brain age gap as a response variable in linear models and tested for associations with
265 psychopathology and cognitive abilities in the HBN sample (N=941, age: 8.01–17.5 years,
266 63.5% males, where 446 subjects from the test set was excluded due to missing clinical

267 (N=325), or cognitive (N=120) values or information on sex (N=1)). In addition to the HBN
268 test sample, we performed the same analysis for the 10% of individuals initially excluded
269 from the PNC sample (N=126; age: 9.5–22.9 years, 39.7% males) and combined the brain age
270 estimates from the N=126 individuals with brain age estimates obtained through cross-
271 validation in the rest of the PNC sample. We performed analyses using BAG scores and
272 tested for associations between BAG and covariates using linear regression models. HBN
273 models were adjusted for age, age-orthogonalized age squared (age^2 , using the poly function
274 in R), sex, tSNR, motion and scanning site, while PNC was adjusted for age, age-
275 orthogonalized age squared (age^2 , using the poly function in R), sex, motion and tSNR.

276

277 Results

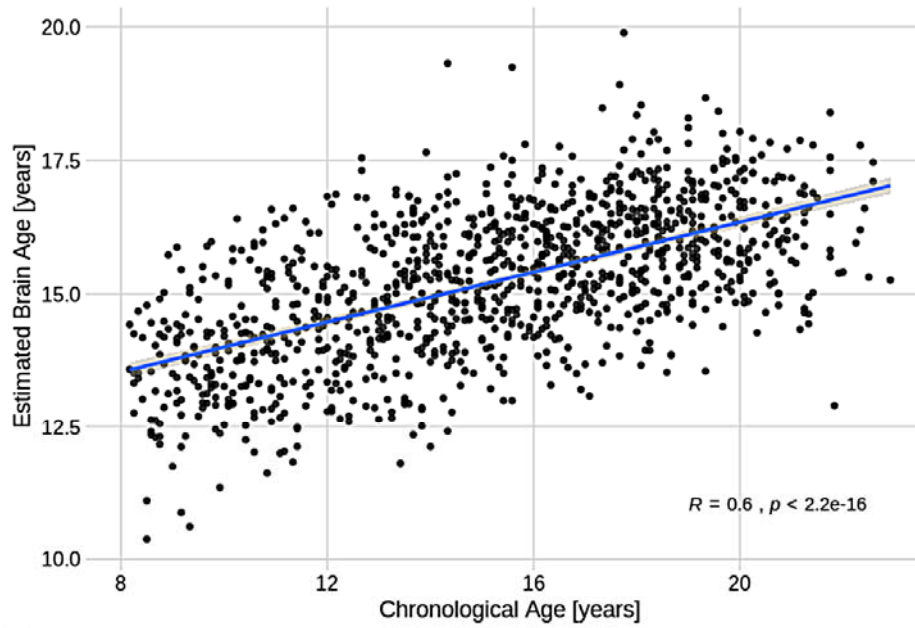
278 The correlation between the estimated brain age and the chronological age, computed through
279 10-fold cross-validation in the training set (PNC), was $r=0.60$ [95% CI: 0.56, 0.63] (fig.1), the
280 mean absolute error (MAE) was 2.43 years and root mean square error (RMSE) was 2.93
281 years, confirming the utility of the functional connectivity features for predicting age. The slm
282 model explained 11.2% of the variance. Figure 2 depicts the feature ranking by use of
283 Correlation-Adjusted (marginal) correlation (CAR) scores from the model giving a measure
284 of variable importance. The top 10 most important edges were between a sensorimotor
285 (SM;IC1) and right SM node (IC2), right SM node (IC2) and left SM node (IC3), Visual
286 Medial node (VM;IC6) and VM (IC8), Default Mode Network (DMN;IC12) and precuneus
287 with frontal gyrus (IC13), thalamus (IC14) and putamen/left insular cortex (IC19), thalamus
288 (IC15) and cerebellar node (IC46), precuneus and posterior cingulate (IC17) with cerebellar
289 node (IC46), superior parietal lobe and SM regions (IC5) with Juxtapositional lobule and
290 cingulate gyrus (IC59), VM (IC6), with Juxtapositional lobule, precentral and middle frontal

291 gyrus (IC76), as well as lateral occipital cortex, and pre/postcentral gyrus (IC50) and VO

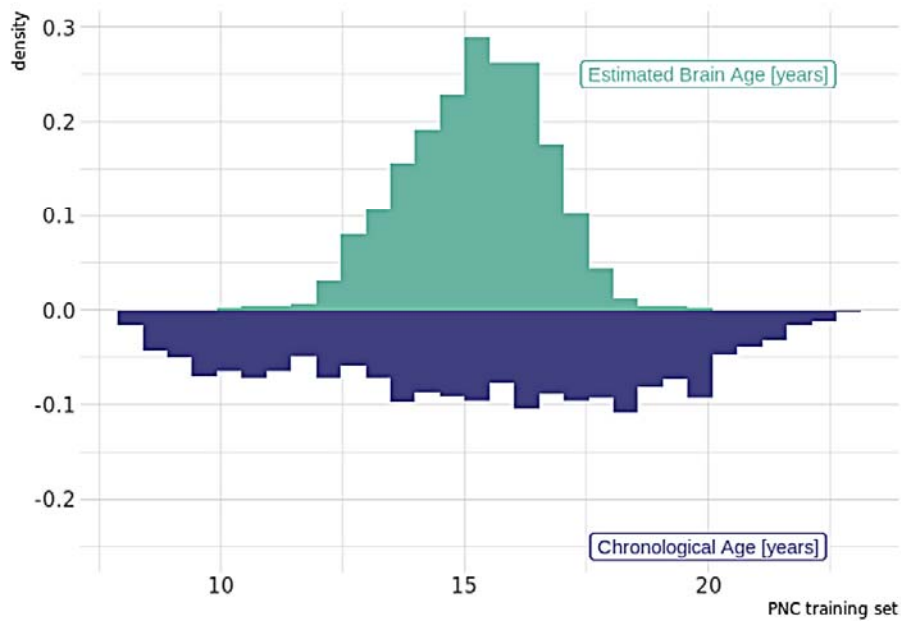
292 (IC86).

293

A Training set: PNC



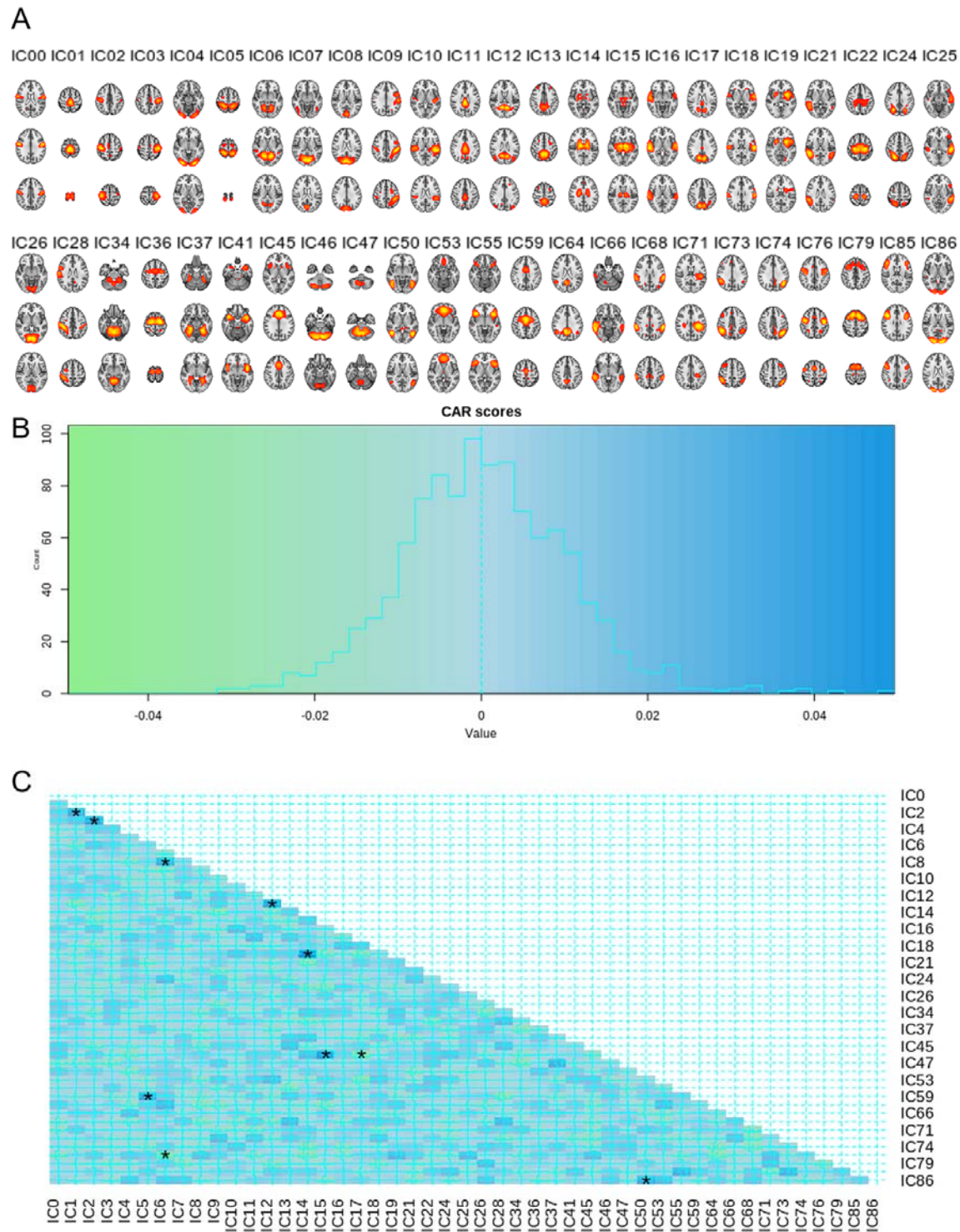
B



294

295 FIG1: A) Model performance for the training set (PNC) where the Pearson correlation
296 between estimated and real age is $r=0.60$. B) Density plot showing the distributions of
297 chronological age and estimated brain age for the training set.

298



299

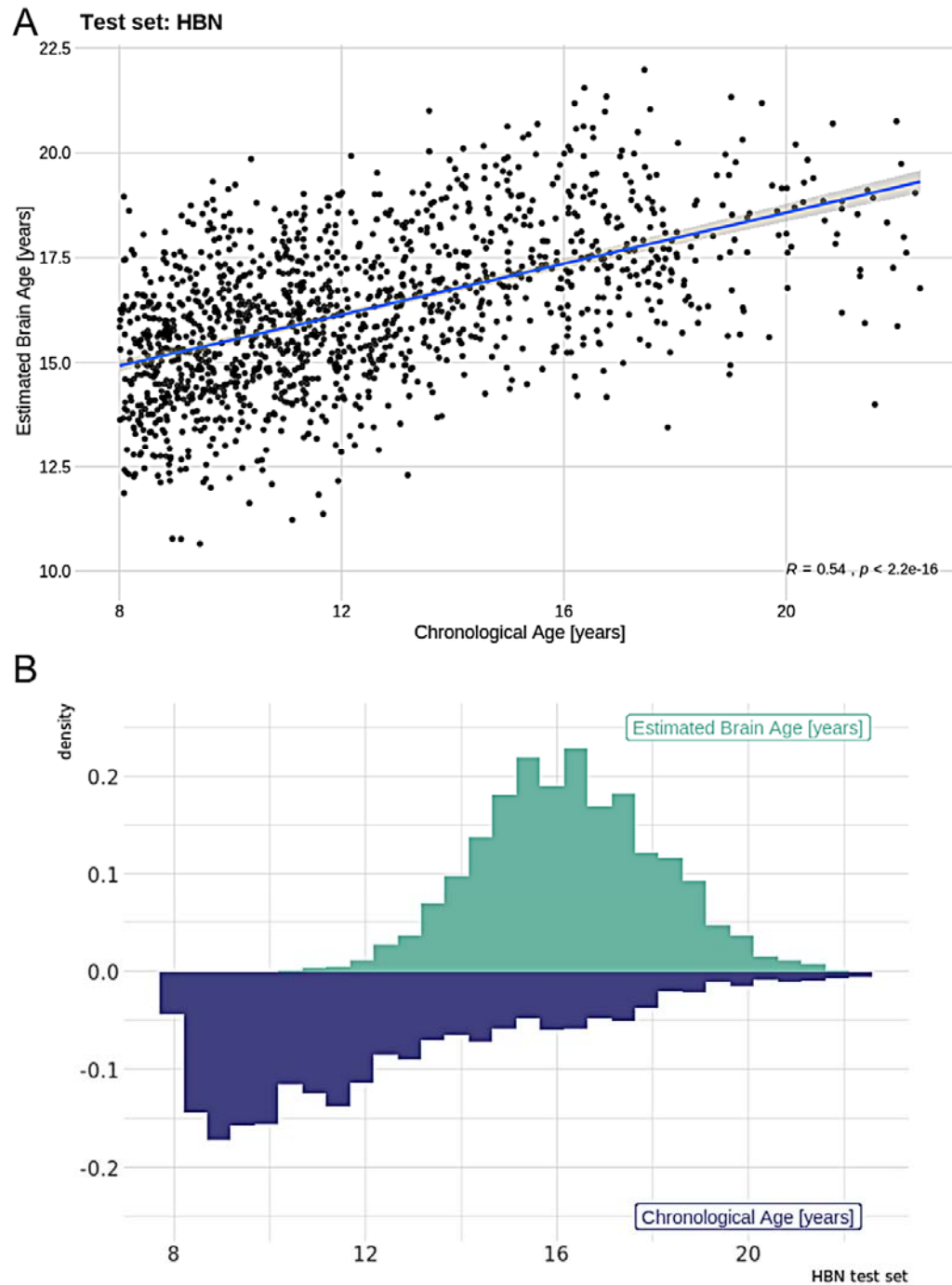
300 FIG2: A) The components from the meta-ICA that were included for the analysis. B)
301 Distribution of CAR scores. As expected, the dependencies are low given that we used a
302 partial correlation framework with regularization in FSLNets to estimate connectivity. C)

303 CAR score matrix showing the dependencies among predictors, where the 10 most important
304 features calculated from the correlation between the response and the Mahalanobis-
305 decorrelated predictors are marked with a star.

306

307 Next, we applied the PNC model to independent test data from the HBN sample. The
308 correlation between chronological age and estimated brain age was $r = 0.54$ [95% CI: 0.50,
309 0.57] (fig.3), MAE was 4.24 years and RMSE = 4.79 years. While these errors were higher
310 than the errors within the PNC sample, considering the test sample comes from different
311 scanners these results nonetheless confirmed the validity of the model, illustrating high
312 consistency between samples and scanners. For further investigation of scanning site effects,
313 we examined model performance for each site. We found that the correlation between the
314 estimated brain age and the chronological age for the scanner located in Staten Island
315 (N=272) was $r = 0.64$ [95% CI: 0.56, 0.71], the MAE was 3.46 years and RMSE= 4.03 years.
316 For Rutgers (N=584), the correlation was $r = 0.58$ [95% CI: 0.53, 0.64], the MAE was 4.87
317 years and RMSE= 5.36 years, while for CBIC (N=531) $r = 0.55$ [95% CI: 0.49, 0.61], the MAE
318 was 3.95 years and RMSE= 4.47 years. This shows that there is some variability between
319 sites, but that the model overall performs similarly across sites. We therefore dealt with site
320 effects by incorporating it as a fixed factor in the association analyses. The model
321 performance across sites also underlines the feasibility of the meta-ICA framework to derive
322 robust functional networks in data from different scanners, yielding compatible whole-brain
323 networks across sites.

324



325

326 FIG3: A) Model performance for the test set (HBN) where the Pearson correlation between
327 estimated and real age is $r=0.54$. B) Density plot showing the distribution between
328 chronological age and estimated brain age for the training sample.

329

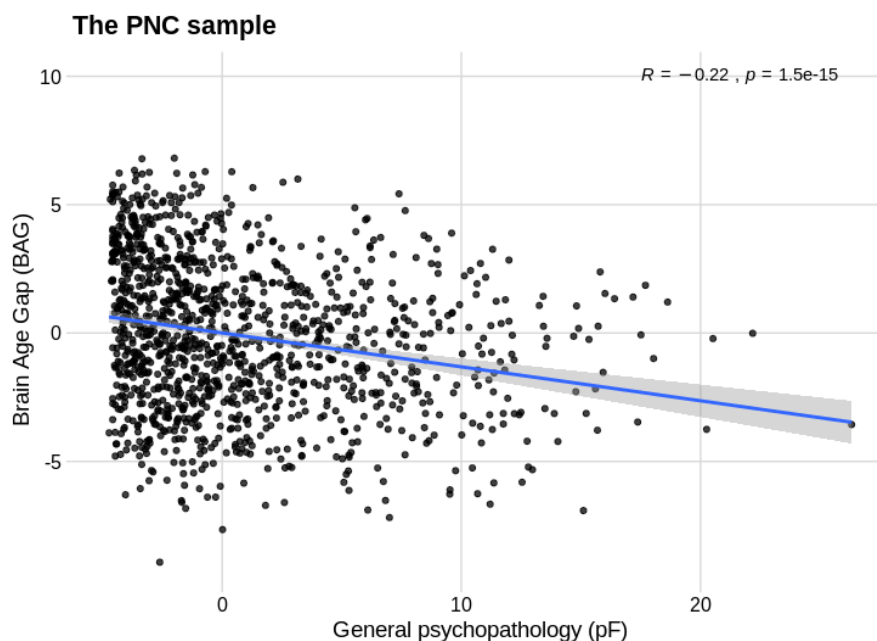
330 Linear models revealed no significant associations for BAG and mental health (pF : $t=-0.11$,
331 $P=.91$, pF_2 : $t=-0.55$, $P=.58$) or cognitive abilities ($t=0.95$, $P=.34$) in the test set, when
332 accounting for age, age-orthogonalized age squared, sex, $tSNR$, motion and scanning site. In
333 line with earlier research, there were significant associations between BAG and age, motion
334 and scanning site (see supplementary table 1). We tested for interaction effects of cognitive
335 abilities and chronological age, but we did not find that cognitive abilities depend on age, or
336 influences the association with the brain age gap ($FSIQ*Chronological\ Age$: $t=0.1$, $P=.92$).

337

338 Additionally, using the existing PNC model, we estimated brain age for the 10% of the PNC
339 participants ($N=126$) with the highest mental health burden that were excluded from the
340 training set. The correlation between chronological age and estimated brain age in this small
341 sample was $r= 0.42$ [95% CI: 0.27, 0.56], MAE was 2.26 years and RMSE = 2.81 years.
342 Next, we merged the brain age estimates from the $N=126$ individuals with the brain age
343 estimates computed in a cross-validation framework run within the training set, yielding
344 estimates for all individuals in the PNC sample ($N=1252$). Using the full sample, we tested
345 for associations with pF and a g factor (gF for PNC was estimated based on the instruments
346 given here; Alnæs et al. (2018)), accounting for age, age-orthogonalized age squared, sex,
347 motion and $tSNR$, using a linear model. We observed a significant association between
348 mental health and BAG ($t=-2.8$, $P<.01$). Specifically, higher symptom burden was associated
349 with lower BAG, indicating that individuals with a younger (estimated) brain age compared
350 to chronological age had a higher level of psychiatric symptoms (fig.4). We found no
351 significant associations for BAG and cognitive abilities ($t=1.59$, $P>.1$).

352

353



354

355 FIG4: Plot showing the significant negative association of psychopathology (pF) and Brain
356 Age Gap (BAG) for the full PNC sample (N=1252).

357

358 Discussion

359 Here, we performed age prediction using machine learning on functional connectivity derived
360 from resting state data (rsfMRI), allowing us to reduce a sizeable amount of data to a single
361 measure of estimated functional brain age per individual. As rsfMRI does not include a
362 cognitively demanding task or require a long scan duration, this is an appealing method for
363 collecting data across individuals with different disorders. The absence of a specific task
364 protocol also makes it ideally suited to combine data from different samples, thereby meeting
365 the requirements for large samples to obtain robust machine learning models. Indeed, we here
366 show that brain age models trained on functional connectivity of one sample can be
367 successfully applied to other samples, even though predictions regress towards the mean of
368 the training set (Fig. 3b), including those with data obtained from different scanners and
369 protocols. A correlation of around 0.6 between chronological age and estimated brain age for

370 different sites was consistent with other studies estimating brain age using functional
371 connectivity as feature input (Li et al., 2018; Truelove-Hill et al., 2020). The moderate
372 correlation is expected as the functional connectome is highly dynamic over the lifespan and
373 across contexts. However, a developmental pattern encompassing a core functional
374 connectome backbone in rsfMRI data has shown high test-retest reliability (Thomason et al.,
375 2011; Zuo & Xing, 2014), and reproducible inter- and intra-subject rsfMRI measures
376 (Damoiseaux et al., 2006; Shehzad et al., 2009). As such, despite moderate correlations the
377 models are likely to capture biologically relevant information, and may be used to indicate
378 trajectories for typical and non-typical brain development and neural restructuring important
379 for susceptibility to brain disorders.

380

381 The brain age approach allowed us to assess the relationship between an estimated brain age
382 gap and cognition and mental health in independent data, while our dimensional approach to
383 mental health data enabled us to characterize both healthy subjects and individuals with a
384 psychiatric disorder along a symptom dimension, rather than applying a binary distinction as
385 cases and controls. Such dimensional approaches may more aptly identify phenotypes which
386 map to brain biology and the neuronal mechanisms underlying the symptoms than diagnostic
387 categories (Hengartner & Lehmann, 2017; Krueger & Bezdjian, 2009).

388

389 Our hypothesis of a link between functional brain age gap, a proxy for brain maturation, and
390 psychopathology was supported in PNC but not in the HBN sample. The significant
391 association between general psychopathology and BAG in the PNC sample, where a higher
392 symptom burden was associated with a lower BAG, is in accordance with studies showing a
393 delay in brain maturation being linked to poorer mental health in the same sample (Kaufmann
394 et al., 2017) and also in young patients with schizophrenia (Douaud et al., 2009). Whether

395 mental health is associated with a higher or lower BAG may largely depend on its timing.
396 While work in youths' points to a lower BAG with increased symptoms (interpreted as a
397 delayed development), work in adults has shown a higher BAG with disorders (interpreted as
398 apparent aging). For example, studies estimating structural brain age in 16-22 years old
399 individuals has shown higher brain age for schizophrenia patients compared to controls
400 (Truelove-Hill et al., 2020), consistent with studies in adults (Kaufmann et al., 2019;
401 Koutsouleris et al., 2013), illustrating that both structural and functional brain age models
402 capture important patterns. As such, the lack of significant associations in HBN could be
403 related to a number of factors, including that the pF captures different aspects of mental health
404 in the two samples, that HBN samples from the point of transition between decreased BAG
405 (childhood) and increased BAG (adulthood), or that there is no difference due to mental
406 health. Alternatively, it is possible that the linear machine learning model did not have
407 enough flexibility to detect non-linear effects in development. It will be interesting in future
408 research to see if models that do better at capturing non-linear maturation trajectories may
409 reveal associations with psychopathology.

410

411 Contrary to our expectations, our analysis revealed no significant associations between BAG
412 and cognitive test performance. In contrast, previous work utilizing the PNC sample have
413 observed that individual differences in working memory performance is linked with the
414 centrality of the cingulo-opercular network (Kolskar et al., 2018). Moreover, for
415 developmental trajectories in youths, it has been illustrated that networks associated with
416 cognition and emotion have locally increased functional connectivity compared to adults,
417 indicating fine-tuning and specialization occurring during the first years of adolescence,
418 principally in networks characterized for higher-order cognitive functioning (Hoff, Van den
419 Heuvel, Benders, Kersbergen, & De Vries, 2013). Also, for adults, permutation tests showed

420 above chance-level prediction accuracy for trait-level educational attainment and fluid
421 intelligence in rsfMRI data from UK Biobank. Both variables were negatively linked with
422 functional connectivity in frontal and default mode networks (Maglanoc et al., 2020). In
423 relation to disorders, differences have been found in functional connectivity for the putamen,
424 dorsal and default-mode regions in Alzheimer’s disease in comparison with mild cognitive
425 and subjective cognitive impairment (Cordova-Palomera et al., 2017). Likewise, anatomical
426 BAG has been associated with sex, with females developing earlier than males (Brouwer et
427 al., 2020), yet there was no significant association with sex for the functional BAGs in our
428 current study. This could be due to not training the model separately for females and males,
429 owing to limitations in number of features versus participants. Still, the model performance
430 showed that shared variability for both sexes was captured.

431

432 Apart from the investigations into BAG, we identified a set of specific connections important
433 for modeling brain age. Central features for the brain age prediction included sensorimotor,
434 visual, insular, DMN, cerebellar and language processing regions, which is coherent with
435 changes in sensory, motor and cognitive abilities observed across this age span (Casey,
436 Tottenham, Liston, & Durston, 2005; de Bie et al., 2012). Our findings are in line with
437 reviews (Power, Fair, Schlaggar, & Petersen, 2010; Uddin, Supekar, & Menon, 2010)
438 showing alterations in these functional connectivity patterns in development. Specifically,
439 studies have shown that brain maturation in children and adolescence may involve a decrease
440 in connectivity of short-range connections and an increase of long-range connections in
441 functional networks. This has been observed for instance in a reduction in short-length
442 connections for the SM and anterior cingulate cortex in young children (Kelly et al., 2008;
443 Supekar, Musen, & Menon, 2009), and for segregation of frontal regions and the DMN in late
444 childhood (Fair et al., 2009).

445

446 Conclusions

447 In the present study, we estimated functional brain connectivity from rsfMRI data from
448 children and adolescents, and used connectivity strengths as features for brain age prediction.
449 Our model showed reasonable performance, and consistency across samples and scanning
450 sites. The most important connections for age prediction were related to sensorimotor, visual,
451 insular, DMN, cerebellar and language areas, indicating that these neural circuits are central
452 in adolescent development. While we found mixed results for behavioral and clinical
453 associations of the brain age gap, the applicability of models to data from different sites
454 supports the utility of the brain age prediction framework for multisite investigations.

455

456 Funding

457 The authors were funded by the Research Council of Norway #276082 (LifespanHealth),
458 #223273 (NORMENT), #249795, #298646, #300767, #283798; H2020 European Research
459 Council #802998 (BRAINMINT); The South-East Norway Regional Health Authority
460 #2019101, #2019107, #2020086; the Swiss National Science Foundation #PZ00P3_193658.

461

462 Financial disclosures

463 OAA is a consultant for HealthLytix.

464

465 Data and code availability

466 The data incorporated in this work were gathered from the open access Healthy Brain
467 Network and The Philadelphia Neurodevelopmental Cohort resource.

468

469 Acknowledgements

470 This manuscript was prepared using a limited access dataset obtained from the Child Mind
471 Institute Biobank, the HBN resource (<http://www.healthybrainnetwork.org>, and the publicly
472 available Philadelphia Neurodevelopmental Cohort
473 (PNC,[http://www.ncbi.nlm.nih.gov/projects/gap/cgi-
474 bin/study.cgi?study_id=phs000607.v1.p1](http://www.ncbi.nlm.nih.gov/projects/gap/cgi-bin/study.cgi?study_id=phs000607.v1.p1)) with permission no.8642. Support for the
475 collection of the PNC data set was provided by grant #RC2MH089983 awarded to Raquel
476 Gur, MD, PhD, and #RC2MH089924 awarded to Hakon Hakonarson, MD, PhD. All PNC
477 participants were recruited through the Center for Applied Genomics at The Children's
478 Hospital in Philadelphia.

479 This manuscript reflects the views of the authors and does not necessarily reflect the opinions
480 or views of any other agency, organization, employer or company. This work was performed
481 on the TSD (Tjeneste for Sensitive Data) facilities, owned by the University of Oslo, operated
482 and developed by the TSD service group at the University of Oslo, IT-Department (USIT)
483 (tsd-drift@usit.uio.no).

484

485

486 References

487

- 488 Alexander, L. M., Escalera, J., Ai, L., Andreotti, C., Febre, K., Mangone, A., . . . Milham, M.
489 P. (2017). An open resource for transdiagnostic research in pediatric mental health and
490 learning disorders. *Scientific Data*, 4(1). doi:10.1038/sdata.2017.181
491 Alexander, L. M., Salum, G. A., Swanson, J. M., & Milham, M. P. (2020). Measuring
492 strengths and weaknesses in dimensional psychiatry. *J Child Psychol Psychiatry*,
493 61(1), 40-50. doi:10.1111/jcpp.13104
494 Alnaes, D., Kaufmann, T., van der Meer, D., Cordova-Palomera, A., Rokicki, J., Moberget,
495 T., . . . Karolinska Schizophrenia Project, C. (2019). Brain Heterogeneity in
496 Schizophrenia and Its Association With Polygenic Risk. *JAMA Psychiatry*, 76(7), 739-
497 748. doi:10.1001/jamapsychiatry.2019.0257
498 Alnaes, D., Kaufmann, T., Doan, N. T., Córdoba-Palomera, A., Wang, Y., Bettella, F., . . .
499 Westlye, L. T. (2018). Association of Heritable Cognitive Ability and
500 Psychopathology With White Matter Properties in Children and Adolescents. *JAMA*
501 *psychiatry*, 75(3), 287-295. doi:10.1001/jamapsychiatry.2017.4277

- 502 Beckmann, C. F., & Smith, S. M. (2004). Probabilistic Independent Component Analysis for
503 Functional Magnetic Resonance Imaging. *IEEE Transactions on Medical Imaging*,
504 23(2), 137-152. doi:10.1109/tmi.2003.822821
- 505 Besenek, M. (2020). Anterior cingulate cortex disconnectivity in high-risk offspring of
506 bipolar patients: a preliminary DTI study. *Dusunen Adam: The Journal of Psychiatry*
507 *and Neurological Sciences*. doi:10.14744/dajpns.2019.00030
- 508 Brouwer, R. M., Schutte, J., Janssen, R., Boomsma, D. I., Hulshoff Pol, H. E., & Schnack, H.
509 G. (2020). The Speed of Development of Adolescent Brain Age Depends on Sex and
510 Is Genetically Determined. *Cereb Cortex*. doi:10.1093/cercor/bhaa296
- 511 Calkins, M. E., Merikangas, K. R., Moore, T. M., Burstein, M., Behr, M. A., Satterthwaite, T.
512 D., . . . Gur, R. E. (2015). The Philadelphia Neurodevelopmental Cohort: constructing
513 a deep phenotyping collaborative. *J Child Psychol Psychiatry*, 56(12), 1356-1369.
514 doi:10.1111/jcpp.12416
- 515 Calkins, M. E., Moore, T. M., Merikangas, K. R., Burstein, M., , Satterthwaite, T. D., Bilker,
516 W. B., & Gur, R. E. (2014). The psychosis spectrum in a young US community
517 sample: findings from the Philadelphia Neurodevelopmental Cohort. *World*
518 *Psychiatry*, 13(3), 296-305.
- 519 Cao, H., & Schwarz, E. (2020). Opportunities and challenges of machine learning approaches
520 for biomarker signature identification in psychiatry *Personalized Psychiatry* (pp. 117-
521 126).
- 522 Casey, B. J., Tottenham, N., Liston, C., & Durston, S. (2005). Imaging the developing brain:
523 what have we learned about cognitive development? *Trends Cogn Sci*, 9(3), 104-110.
524 doi:10.1016/j.tics.2005.01.011
- 525 Caspi, A., Houts, R. M., Belsky, D. W., Goldman-Mellor, S. J., Harrington, H., Israel, S., . . .
526 Moffitt, T. E. (2013). The p Factor. *Clinical Psychological Science*, 2(2), 119-137.
527 doi:10.1177/2167702613497473
- 528 Chung, Y., Addington, J., Bearden, C. E., Cadenhead, K., Cornblatt, B., Mathalon, D. H., . . .
529 Genetics Study, C. (2018). Use of Machine Learning to Determine Deviance in
530 Neuroanatomical Maturity Associated With Future Psychosis in Youths at Clinically
531 High Risk. *JAMA Psychiatry*, 75(9), 960-968. doi:10.1001/jamapsychiatry.2018.1543
- 532 Collin, G., Seidman, L. J., Keshavan, M. S., Stone, W. S., Qi, Z., Zhang, T., . . . Whitfield-
533 Gabrieli, S. (2020). Functional connectome organization predicts conversion to
534 psychosis in clinical high-risk youth from the SHARP program. *Mol Psychiatry*,
535 25(10), 2431-2440. doi:10.1038/s41380-018-0288-x
- 536 Cordova-Palomera, A., Kaufmann, T., Persson, K., Alnaes, D., Doan, N. T., Moberget, T., . . .
537 Westlye, L. T. (2017). Disrupted global metastability and static and dynamic brain
538 connectivity across individuals in the Alzheimer's disease continuum. *Sci Rep*, 7,
539 40268. doi:10.1038/srep40268
- 540 Craddock, N., & Owen, M. J. (2010). The Kraepelinian dichotomy - going, going... but still
541 not gone. *Br J Psychiatry*, 196(2), 92-95. doi:10.1192/bjp.bp.109.073429
- 542 Cropley, V. L., Tian, Y., Fernando, K., Mansour, L. S., Pantelis, C., Cocchi, L., & Zalesky,
543 A. (2020). Brain-Predicted Age Associates With Psychopathology Dimensions in
544 Youths. *Biol Psychiatry Cogn Neurosci Neuroimaging*.
545 doi:10.1016/j.bpsc.2020.07.014
- 546 Damoiseaux, J. S., Rombouts, S. A., Barkhof, F., Scheltens, P., Stam, C. J., Smith, S. M., &
547 Beckmann, C. F. (2006). Consistent resting-state networks across healthy subjects.
548 *Proc Natl Acad Sci U S A*, 103(37), 13848-13853. doi:10.1073/pnas.0601417103
- 549 de Bie, H. M., Boersma, M., Adriaanse, S., Veltman, D. J., Wink, A. M., Roosendaal, S. D., .
550 . . . Sanz-Arigitia, E. J. (2012). Resting-state networks in awake five- to eight-year old
551 children. *Hum Brain Mapp*, 33(5), 1189-1201. doi:10.1002/hbm.21280

- 552 de Lange, A. G., Anaturk, M., Suri, S., Kaufmann, T., Cole, J. H., Griffanti, L., . . . Ebmeier,
553 K. P. (2020). Multimodal brain-age prediction and cardiovascular risk: The Whitehall
554 II MRI sub-study. *NeuroImage*, *222*, 117292. doi:10.1016/j.neuroimage.2020.117292
- 555 Dosenbach, N. U. F., Nardos, B., Cohen, A. L., Fair, D. A., Power, J. D., Church, J. A., . . .
556 Schlaggar, B. L. (2010). Prediction of Individual Brain Maturity Using fMRI. *Science*,
557 *329*(5997), 1358-1361. doi:10.1126/science.1194144
- 558 Douaud, G., Mackay, C., Andersson, J., James, S., Quested, D., Ray, M. K., . . . James, A.
559 (2009). Schizophrenia delays and alters maturation of the brain in adolescence. *Brain*,
560 *132*(Pt 9), 2437-2448. doi:10.1093/brain/awp126
- 561 Fair, D. A., Cohen, A. L., Power, J. D., Dosenbach, N. U., Church, J. A., Miezin, F. M., . . .
562 Petersen, S. E. (2009). Functional brain networks develop from a "local to distributed"
563 organization. *PLoS Comput Biol*, *5*(5), e1000381. doi:10.1371/journal.pcbi.1000381
- 564 Franke, K., Luders, E., May, A., Wilke, M., & Gaser, C. (2012). Brain maturation: predicting
565 individual BrainAGE in children and adolescents using structural MRI. *NeuroImage*,
566 *63*(3), 1305-1312. doi:10.1016/j.neuroimage.2012.08.001
- 567 Franke, K., Ziegler, G., Kloppel, S., Gaser, C., & Alzheimer's Disease Neuroimaging, I.
568 (2010). Estimating the age of healthy subjects from T1-weighted MRI scans using
569 kernel methods: exploring the influence of various parameters. *NeuroImage*, *50*(3),
570 883-892. doi:10.1016/j.neuroimage.2010.01.005
- 571 Griffanti, L., Salimi-Khorshidi, G., Beckmann, C. F., Auerbach, E. J., Douaud, G., Sexton, C.
572 E., . . . Smith, S. M. (2014). ICA-based artefact removal and accelerated fMRI
573 acquisition for improved resting state network imaging. *NeuroImage*, *95*, 232-247.
574 doi:10.1016/j.neuroimage.2014.03.034
- 575 Gur, R. C., Calkins, M. E., Satterthwaite, T. D., Ruparel, K., Bilker, W. B., Moore, T. M., . . .
576 Gur, R. E. (2014). Neurocognitive growth charting in psychosis spectrum youths.
577 *JAMA Psychiatry*, *71*(4), 366-374. doi:10.1001/jamapsychiatry.2013.4190
- 578 Hengartner, M. P., & Lehmann, S. N. (2017). Why Psychiatric Research Must Abandon
579 Traditional Diagnostic Classification and Adopt a Fully Dimensional Scope: Two
580 Solutions to a Persistent Problem. *Front Psychiatry*, *8*, 101.
581 doi:10.3389/fpsy.2017.00101
- 582 Hoff, G. E., Van den Heuvel, M. P., Benders, M. J., Kersbergen, K. J., & De Vries, L. S.
583 (2013). On development of functional brain connectivity in the young brain. *Front*
584 *Hum Neurosci*, *7*, 650. doi:10.3389/fnhum.2013.00650
- 585 Hyvärinen, A. (1999). Fast and robust fixed-point algorithms for independent component
586 analysis. *IEEE Transactions on Neural Networks*, *10*(3), 626-634.
- 587 Insel, T. R. (2010). Rethinking schizophrenia. *Nature*, *468*(7321), 187-193.
588 doi:10.1038/nature09552
- 589 Jenkinson, M., Bannister, P., Brady, M., & Smith, S. (2002). Improved Optimization for the
590 Robust and Accurate Linear Registration and Motion Correction of Brain Images.
591 *NeuroImage*, *17*(2), 825-841. doi:10.1006/nimg.2002.1132
- 592 Jollans, L., & Whelan, R. (2018). Neuromarkers for Mental Disorders: Harnessing Population
593 Neuroscience. *Front Psychiatry*, *9*, 242. doi:10.3389/fpsy.2018.00242
- 594 Kassani, P. H., Gossman, A., & Wang, Y. P. (2020). Multimodal Sparse Classifier for
595 Adolescent Brain Age Prediction. *IEEE J Biomed Health Inform*, *24*(2), 336-344.
596 doi:10.1109/JBHI.2019.2925710
- 597 Kaufmann, T., Alnæs, D., Doan, N. T., Brandt, C. L., Andreassen, O. A., & Westlye, L. T.
598 (2017). Delayed stabilization and individualization in connectome development are
599 related to psychiatric disorders. *Nat Neurosci*, *20*(4), 513-515. doi:10.1038/nn.4511

- 600 Kaufmann, T., Elvsashagen, T., Alnaes, D., Zak, N., Pedersen, P. O., Norbom, L. B., . . .
601 Westlye, L. T. (2016). The brain functional connectome is robustly altered by lack of
602 sleep. *NeuroImage*, *127*, 324-332. doi:10.1016/j.neuroimage.2015.12.028
- 603 Kaufmann, T., van der Meer, D., Doan, N. T., Schwarz, E., Lund, M. J., Agartz, I., . . .
604 Westlye, L. T. (2019). Common brain disorders are associated with heritable patterns
605 of apparent aging of the brain. *Nature Neuroscience*, *22*(10), 1617-1623.
606 doi:10.1038/s41593-019-0471-7
- 607 Kelly, A. M. C., Di Martino, A., Uddin, L. Q., Shehzad, Z., Gee, D. G., Reiss, P. T., . . .
608 Milham, M. P. (2008). Development of Anterior Cingulate Functional Connectivity
609 from Late Childhood to Early Adulthood. *Cerebral Cortex*, *19*(3), 640-657.
610 doi:10.1093/cercor/bhn117
- 611 Kolskar, K. K., Alnaes, D., Kaufmann, T., Richard, G., Sanders, A. M., Ulrichsen, K. M., . . .
612 Westlye, L. T. (2018). Key Brain Network Nodes Show Differential Cognitive
613 Relevance and Developmental Trajectories during Childhood and Adolescence.
614 *eNeuro*, *5*(4). doi:10.1523/ENEURO.0092-18.2018
- 615 Koutsouleris, N., Davatzikos, C., Borgwardt, S., Gaser, C., Bottlender, R., Frodl, T., . . .
616 Meisenzahl, E. (2013). Accelerated Brain Aging in Schizophrenia and Beyond: A
617 Neuroanatomical Marker of Psychiatric Disorders. *Schizophrenia Bulletin*, *40*(5),
618 1140-1153. doi:10.1093/schbul/sbt142
- 619 Krueger, R. F., & Bezdjian, S. (2009). Enhancing research and treatment of mental disorders
620 with dimensional concepts: toward DSM-V and ICD-11. . *World Psychiatry*, *8*(1)(3).
- 621 Ledoit, O., & Wolf, M. (2003). Improved estimation of the covariance matrix of stock returns
622 with an application to portfolio selection. *Journal of Empirical Finance*, *10*(5), 603-
623 621. doi:10.1016/s0927-5398(03)00007-0
- 624 Li, H., Satterthwaite, T. D., & Fan, Y. (2018). Brain age prediction based on resting-state
625 functional connectivity patterns using convolutional neural networks. . *In 2018 IEEE*
626 *15th International Symposium on Biomedical Imaging*, 101-104.
627 doi:10.1109/ISBI.2018.8363532
- 628 Lian, N., Lv, H., Guo, W., Shen, Y., Wu, R., Liu, Y., . . . Zhao, J. (2018). A comparative
629 study of magnetic resonance imaging on the gray matter and resting-state function in
630 prodromal and first-episode schizophrenia. *Am J Med Genet B Neuropsychiatr Genet*,
631 *177*(6), 537-545. doi:10.1002/ajmg.b.32644
- 632 Linden, D. E. (2012). The challenges and promise of neuroimaging in psychiatry. *Neuron*,
633 *73*(1), 8-22. doi:10.1016/j.neuron.2011.12.014
- 634 Lund, M. J., Alnaes, D., Schwab, S., van der Meer, D., Andreassen, O. A., Westlye, L. T., &
635 Kaufmann, T. (2020). Differences in directed functional brain connectivity related to
636 age, sex and mental health. *Hum Brain Mapp*. doi:10.1002/hbm.25116
- 637 Lund, M. J., Alnaes, D., Rokicki, J., Schwab, S., Andreassen, O. A., Westlye, L. T., &
638 Kaufmann, T. (2021). Functional connectivity directionality between large-scale
639 resting-state networks in children and adolescence from the Healthy Brain Network
640 sample. *medRxiv*, 2020-10.
- 641 Maglanoc, L. A., Kaufmann, T., van der Meer, D., Marquand, A. F., Wolfers, T., Jonassen,
642 R., . . . Westlye, L. T. (2020). Brain Connectome Mapping of Complex Human Traits
643 and Their Polygenic Architecture Using Machine Learning. *Biological Psychiatry*,
644 *87*(8), 717-726. doi:10.1016/j.biopsych.2019.10.011
- 645 Mansourvar M., Wiil U.K., & C., N. (2020). *Big Data Analytics in Healthcare: A Review of*
646 *Opportunities and Challenges*. Paper presented at the In International Conference for
647 Emerging Technologies in Computing.
- 648 Miller, K. L., Alfaro-Almagro, F., Bangerter, N. K., Thomas, D. L., Yacoub, E., Xu, J., . . .
649 Smith, S. M. (2016). Multimodal population brain imaging in the UK Biobank

- 650 prospective epidemiological study. *Nature Neuroscience*, 19(11), 1523-1536.
651 doi:10.1038/nn.4393
- 652 Nemeroff, C. B. (2002). Comorbidity of mood and anxiety disorders: the rule, not the
653 exception? *American Journal of Psychiatry*, 159(1), 3-4.
- 654 Owen, M. J. (2014). New approaches to psychiatric diagnostic classification. *Neuron*, 84(3),
655 564-571. doi:10.1016/j.neuron.2014.10.028
- 656 Paulus, M. P., & Thompson, W. K. (2019). The Challenges and Opportunities of Small
657 Effects: The New Normal in Academic Psychiatry. *JAMA Psychiatry*, 76(4), 353-354.
658 doi:10.1001/jamapsychiatry.2018.4540
- 659 Power, J. D., Fair, D. A., Schlaggar, B. L., & Petersen, S. E. (2010). The Development of
660 Human Functional Brain Networks. *Neuron*, 67(5), 735-748.
661 doi:10.1016/j.neuron.2010.08.017
- 662 Pruim, R. H. R., Mennes, M., Buitelaar, J. K., & Beckmann, C. F. (2015). Evaluation of ICA-
663 AROMA and alternative strategies for motion artifact removal in resting state fMRI.
664 *NeuroImage*, 112, 278-287. doi:10.1016/j.neuroimage.2015.02.063
- 665 Pruim, R. H. R., Mennes, M., van Rooij, D., Llera, A., Buitelaar, J. K., & Beckmann, C. F.
666 (2015). ICA-AROMA: A robust ICA-based strategy for removing motion artifacts
667 from fMRI data. *NeuroImage*, 112, 267-277. doi:10.1016/j.neuroimage.2015.02.064
- 668 Rudolph, M. D., Miranda-Dominguez, O., Cohen, A. O., Breiner, K., Steinberg, L., Bonnie,
669 R. J., . . . Fair, D. A. (2017). At risk of being risky: The relationship between "brain
670 age" under emotional states and risk preference. *Dev Cogn Neurosci*, 24, 93-106.
671 doi:10.1016/j.dcn.2017.01.010
- 672 Saito, J., Nemoto, T., Katagiri, N., Hori, M., Tagata, H., Funatogawa, T., . . . Mizuno, M.
673 (2020). Can reduced leftward asymmetry of white matter integrity be a marker of
674 transition to psychosis in at-risk mental state? *Asian J Psychiatr*, 54, 102450.
675 doi:10.1016/j.ajp.2020.102450
- 676 Salimi-Khorshidi, G., Douaud, G., Beckmann, C. F., Glasser, M. F., Griffanti, L., & Smith, S.
677 M. (2014). Automatic denoising of functional MRI data: combining independent
678 component analysis and hierarchical fusion of classifiers. *NeuroImage*, 90, 449-468.
679 doi:10.1016/j.neuroimage.2013.11.046
- 680 Satterthwaite, T. D., Connolly, J. J., Ruparel, K., Calkins, M. E., Jackson, C., Elliott, M. A., . .
681 . Gur, R. E. (2016). The Philadelphia Neurodevelopmental Cohort: A publicly
682 available resource for the study of normal and abnormal brain development in youth.
683 *NeuroImage*, 124(Pt B), 1115-1119. doi:10.1016/j.neuroimage.2015.03.056
- 684 Satterthwaite, T. D., Elliott, M. A., Ruparel, K., Loughhead, J., Prabhakaran, K., Calkins, M.
685 E., . . . Gur, R. E. (2014). Neuroimaging of the Philadelphia neurodevelopmental
686 cohort. *NeuroImage*, 86, 544-553. doi:10.1016/j.neuroimage.2013.07.064
- 687 Schnack, H. G., van Haren, N. E. M., Nieuwenhuis, M., Hulshoff Pol, H. E., Cahn, W., &
688 Kahn, R. S. (2016). Accelerated Brain Aging in Schizophrenia: A Longitudinal
689 Pattern Recognition Study. *American Journal of Psychiatry*, 173(6), 607-616.
690 doi:10.1176/appi.ajp.2015.15070922
- 691 Schäfer, J., & Strimmer, K. (2005). A shrinkage approach to large-scale covariance estimation
692 and implications for functional genomics. *Statistical applications in genetics and
693 molecular biology*, 4(1). doi:DOI:10.2202/1544-6115.1175
- 694 Shehzad, Z., Kelly, A. M. C., Reiss, P. T., Gee, D. G., Gotimer, K., Uddin, L. Q., . . . Milham,
695 M. P. (2009). The Resting Brain: Unconstrained yet Reliable. *Cerebral Cortex*,
696 19(10), 2209-2229. doi:10.1093/cercor/bhn256
- 697 Smith, S. M., Beckmann, C. F., Andersson, J., Auerbach, E. J., Bijsterbosch, J., Douaud, G., .
698 . . Consortium, W. U.-M. H. (2013). Resting-state fMRI in the Human Connectome
699 Project. *NeuroImage*, 80, 144-168. doi:10.1016/j.neuroimage.2013.05.039

- 700 Supekar, K., Musen, M., & Menon, V. (2009). Development of large-scale functional brain
701 networks in children. *PLoS Biol*, 7(7), e1000157. doi:10.1371/
702 Thomason, M. E., Dennis, E. L., Joshi, A. A., Joshi, S. H., Dinov, I. D., Chang, C., . . . Gotlib,
703 I. H. (2011). Resting-state fMRI can reliably map neural networks in children.
704 *NeuroImage*, 55(1), 165-175. doi:10.1016/j.neuroimage.2010.11.080
705 Truelove-Hill, M., Erus, G., Bashyam, V., Varol, E., Sako, C., Gur, R. C., . . . Davatzikos, C.
706 (2020). A Multidimensional Neural Maturation Index Reveals Reproducible
707 Developmental Patterns in Children and Adolescents. *J Neurosci*, 40(6), 1265-1275.
708 doi:10.1523/JNEUROSCI.2092-19.2019
709 Uddin, L. Q., Supekar, K., & Menon, V. (2010). Typical and atypical development of
710 functional human brain networks: insights from resting-state FMRI. *Front Syst*
711 *Neurosci*, 4, 21. doi:10.3389/fnsys.2010.00021
712 Wechsler, D. (2003). *Wechsler intelligence scale for children--Fourth Edition (WISC-IV)*
713 Zhai, J., & Li, K. (2019). Predicting Brain Age Based on Spatial and Temporal Features of
714 Human Brain Functional Networks. *Front Hum Neurosci*, 13, 62.
715 doi:10.3389/fnhum.2019.00062
716 Zuo, X. N., & Xing, X. X. (2014). Test-retest reliabilities of resting-state FMRI
717 measurements in human brain functional connectomics: a systems neuroscience
718 perspective. *Neurosci Biobehav Rev*, 45, 100-118.
719 doi:10.1016/j.neubiorev.2014.05.009
720